Design and Evaluation of an Active Ripple Filter Using Voltage Injection

ALBERT C. CHOW AND DAVID J. PERREAULT

MASSACHUSETTS INSTITUTE OF TECHNOLOGY
LABORATORY FOR ELECTROMAGNETIC AND ELECTRONIC SYSTEMS
CAMBRIDGE, MA 02139 USA

***Abstract*— Active ripple filters can affect substantial reductions in power converter input and output ripple components, allowing considerable reduction in passive component size. This paper investigates a hybrid passive/active filter topology that achieves ripple reduction by injecting a compensating voltage ripple across a series filter element. Both ripple feedforward and feedback are employed. The design of sensor, amplifier, and injector circuitry suitable for the application are investigated. The experimental results demonstrate the feasibility and high performance of the new approach, and illustrate its potential benefits. It is demonstrated that the proposed approach is most effective in cases where it is desirable to minimize the amount of capacitance in the filter.**

I. INTRODUCTION

Switching power converters inherently generate ripple, and typically require input and output filtration to meet ripple and EMI specifications. Passive LC low-pass filters have traditionally been employed to achieve the necessary degree of ripple attenuation [1]. The passive filter components often account for a large portion of converter size, weight, and cost [1-4]. Furthermore the temperature and reliability limitations of filter capacitors can present a significant design constraint.

An alternative to the conventional passive filtering approach is to use a hybrid passive/active filter [2-10]. In this approach, a small passive filter is coupled with an active electronic circuit to attenuate the ripple. The passive filter serves to limit the ripple to a level manageable by the active circuit and attenuate ripple components that fall beyond the bandwidth of the active circuit. The active filter circuit cancels or suppresses the low-frequency ripple components that are most difficult to attenuate with a passive low-pass filter. This approach permits a substantial reduction in the passive filter size, with potential benefits in converter size, weight, and cost.

Active filters may be characterized by whether they inject ripple voltages [3,7] or currents [2,4-10] in the circuit to achieve ripple reduction. Controls governing the ripple correction can be derived through either feedforward [2,9,10] or feedback [5-8]. Feedforward filters sense a ripple component and inject its inverse, while feedback filters suppress ripple via high-gain feedback control. Combinations of these mechanisms are also possible (see [3,4] for example), and there are a wide variety of means for implementing the sensing and injection functions.

This paper focuses on a hybrid passive/active ripple filter topology that achieves ripple reduction by injecting an opposing voltage in series with the voltage ripple source. As illustrated in Fig. 1, the active circuitry injects a voltage opposing the ripple voltage across the buck capacitor C_{buck}; thereby reducing the ripple across C_{out}. The injector design is challenging since it must accurately generate the desired ac injection voltage while carrying the full dc converter current. The injection signal is based on a superposition of easily-measured feedforward and feedback voltage ripple signals. If the feedforward gain is $K(s)$, then the transfer function from the ripple source to the output is

$$\frac{V_{out}(s)}{V_{ripple}(s)} = 1 - K(s) \qquad (1)$$

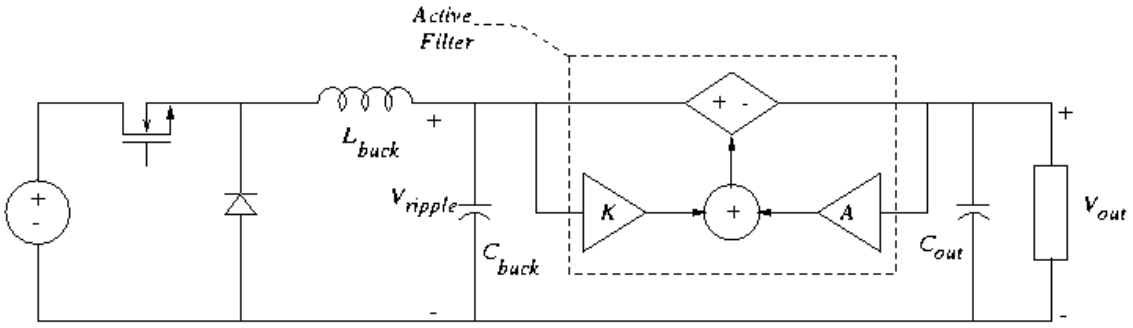

Figure 1 Feedforward / feedback voltage ripple filter used in combination with a passive filter at the output of a buck converter. The hybrid active filter enables a reduction in the size of the passive filter.

For a perfect feedforward path gain of unity, the ripple at the output would be zero. However, due to gain and phase accuracy limitations in the components, feedforward cancellation alone cannot fully attenuate the ripple. Considering the feedback path alone, the ripple source to output transfer function due to feedback becomes:

$$\frac{V_{out}(s)}{V_{ripple}(s)} = \frac{1}{1+A(s)} \qquad (2)$$

which becomes small as the magnitude of gain A(s) increases. In the feedback case, stability considerations limit the achievable feedback suppression. Combining feedforward and feedback takes best advantage of the injector circuitry and maximizes ripple attenuation. It will be shown that the proposed hybrid passive/active filter structure is attractive in cases where it is desirable to minimize the passive filter capacitance.

Section II of the paper explores the design of the proposed active ripple filter. Section III of the paper describes the application of the proposed scheme to the output filter of a buck converter, and compares the performance of the approach to that achievable with a conventional passive filter. Finally, Section IV draws conclusions and presents an evaluation of the proposed approach.

II. ACTIVE FILTER DESIGN

The active filter comprises a voltage injector circuit, a control circuit, and voltage sensors. This section considers each of these subsystems in turn.

A. Voltage Injector Design

The injector circuit (represented as a controlled voltage source in Fig. 1) must meet a number of challenging requirements. First, the injector must carry the full dc output current with minimal losses. Second, the injector must provide both isolation and sufficient input impedance for the active circuitry. Finally, it must be able to replicate the injector signal with high fidelity.

For the given constraints, a transformer proves to be an ideal choice for a voltage injection mechanism [3]. Figure 2 illustrates a transformer-based injector, including the relevant transformer parasitics. The dc current of the converter passes through the magnetizing inductance of the transformer, incurring minimal dc losses. The core must be properly sized and gapped to prevent saturation under this heavy bias condition.

The injected, canceling voltage appears across the magnetizing inductance L_m. The power required to generate this voltage must be supplied by the active circuitry. The transformer magnetizing inductance L_μ and turns ratio must be selected such that the scaled ripple current and voltage can be adequately supplied by the amplifier circuitry. The active circuitry is required to generate an ac voltage of magnitude:

$$V_{circuit} = \frac{N_2}{N_1}\left|V_{ripple}\right| \qquad (3)$$

and a current of magnitude:

$$I_{circuit} = \frac{N_1}{N_2}\frac{\left|V_{ripple}\right|}{w_{ripple}L_u} \qquad (4)$$

where L_m is the magnetizing inductance on the transformer's primary side and ω_{ripple} is the frequency of the ripple. The magnetizing inductance (and hence transfomer core size) is determined by the output current and dissipation limits of the amplifer circuitry. The transformer turns ratio is used to match the voltage and current drive levels of the amplifier circuitry to those required for voltage ripple cancellation. To maximize amplifier use and minimize injector size, the turns ratio should be selected to fully utilize the available amplifier voltage and current swing.

For example, the amplifier circuitry in the prototype system has a voltage limit of +/- 7 V, and a current limit of +/- 100 mA. To suppress a 2.5 volt peak to peak voltage ripple, a turns ratio of 1:5 is selected. For a 125 KHz fundamental ripple frequency a magnetizing inductance of 5 µH is selected so that the current drive capability of the amplifier is not exceeded.

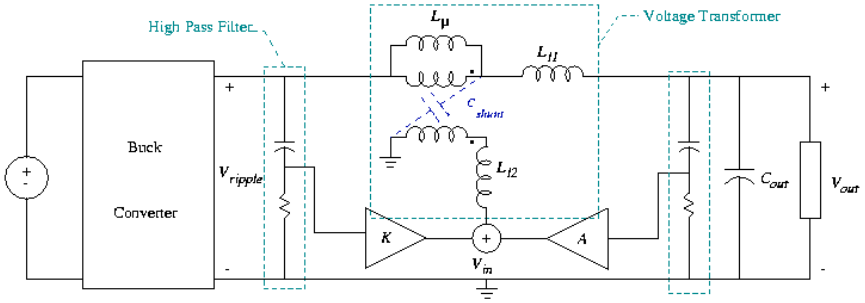

Figure 2 Implementation of the Hybrid Active/Passive Filter. Voltage is sensed with an op amp via a high pass filter. Voltage is injected using a voltage transformer; the significant transformer parasitics are shown. L_m is the magnetizing inductance, and L_{l1} and L_{l2} represent the leakage inductances.

The use of feedforward ripple cancellation requires that the ripple be both sensed and injected with great accuracy. Therefore the injector must have negligible magnitude attenuation and phase shift for the frequency range of interest; any phase or magnitude error will greatly degrade the performance of the feedforward control. For an ideal transformer, the voltage appearing on the primary side is a perfectly scaled version of the voltage on the secondary side. However, transformer parasitics [11,12] (illustrated in Fig. 2) can limit the injector performance. Experimental results have verified that C_{shunt} can be neglected, because it does not affect the behavior of the injector for the frequency range of interest. However, the secondary side leakage inductance, L_{l2}, forms a voltage divider with the secondary side magnetizing inductance, resulting in a magnitude error. A winding geometry that minimizes leakage inductance is advantageous. After investigating several geometries, while keeping implementation ease in mind, an interleaved primary over secondary winding method was selected for the prototype, as this resulted in a low value of L_{l2}.

Stability is a major concern when employing feedback-based ripple attenuation, and is the major factor limiting achievable attenuation. The injector transformer is in the feedback loop, so any phase lag added by the transformer can greatly decrease stability. An ideal transformer adds zero phase lag, but the parasitic inductance on the primary side, L_{l1}, plays a surprisingly important role in the stability of the system. As will be described in Section II, L_{l1} and the output capacitor, C_{out}, form a 2nd order low pass filter, and the phase shift associated with this parasitic filter can affect the stability of the feedback control. As a result, the transformer design should minimize L_{l1} to ease the constraints on the control design. The leakage inductance is dependent on two factors: winding geometry (as mentioned above) and core gap size. Reducing gap size will reduce the leakage inductance, but it substantially increases transformer size.

The main factors that determine transformer size are magnetizing inductance L_m, maximum allowable flux density B_{max}, gap size, maximum current I_{max}, and winding space.

The design of the transformer is highly constrained by the particular application. The maximum current is determined by the converter current rating. The magnetizing inductance is set by the active circuitry constraints of equations 3 and 4. The saturation flux density of the core material B_{sat} and ac losses determine the maximum allowable flux density B_{max}. For a given current, magnetizing inductance, and maximum allowable flux density, there is a direct relationship between A_L (inductance factor nH/turns^2) and core area, A_{core}:

$$A_{core} = \frac{I_{\max}\sqrt{L_m A_L}}{B_{\max}} \qquad (5)$$

A_L is inversely proportional to the gap size, which typically correlates with leakage inductance. Thus, there is a tradeoff between the leakage inductance and the core size. For instance, the prototype injector could be implemented using an RM10 core but with a relatively large gap. To reduce leakage, the prototype injector is built on a larger RM12 core. This results in a primary side leakage (L_{l1}) of 0.156 μH (3.4%). The secondary side leakage (L_{l2}) is 2.3 μH (2.5%). The corresponding attenuation of 9.8 is calculated from eqn. 6.

$$Attenuation = \frac{N^2 L_u}{L_{l1} + N^2 L_u} = \frac{V_{out}}{V_{in}} \qquad (6)$$

B. *Alternative Voltage Injector*

An alternative method for implementing the injector is to use a bypass inductor in parallel with a high-frequency transformer, as illustrated in Fig. 4. In this approach, the bypass inductor, which is implemented with a gapped core and wound with large-gauge wire, serves as the dc bypass element. This function was accomplished by the magnetizing inductance L_m in the previous case. The high frequency transformer is implemented with a significantly smaller ungapped core with small-gauge wire. This element serves as the means for voltage injection. The relative winding resistances determine the dc current sharing between the inductor and the transformer, while the ac characteristics are determined by the relative inductances. The high-frequency transformer must be implemented with a non-gapped core to keep leakage inductances comparable to the single- core

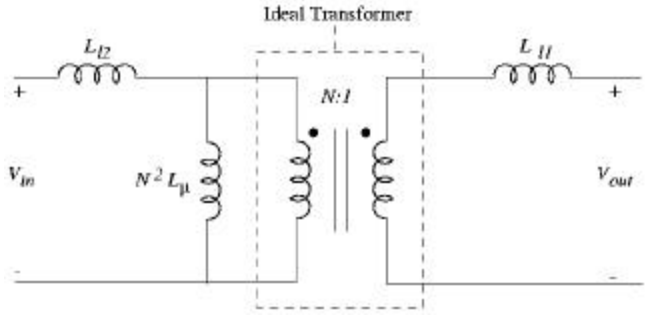

Figure 3 A transformer model including parasitics. The parasitics can cause magnitude and phase errors.

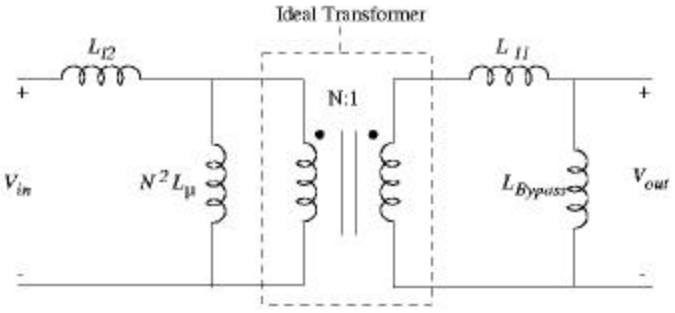

Figure 4 Injector implementation uses a bypass inductor in parallel with an high frequency transformer. The significant parasitics are also represented.

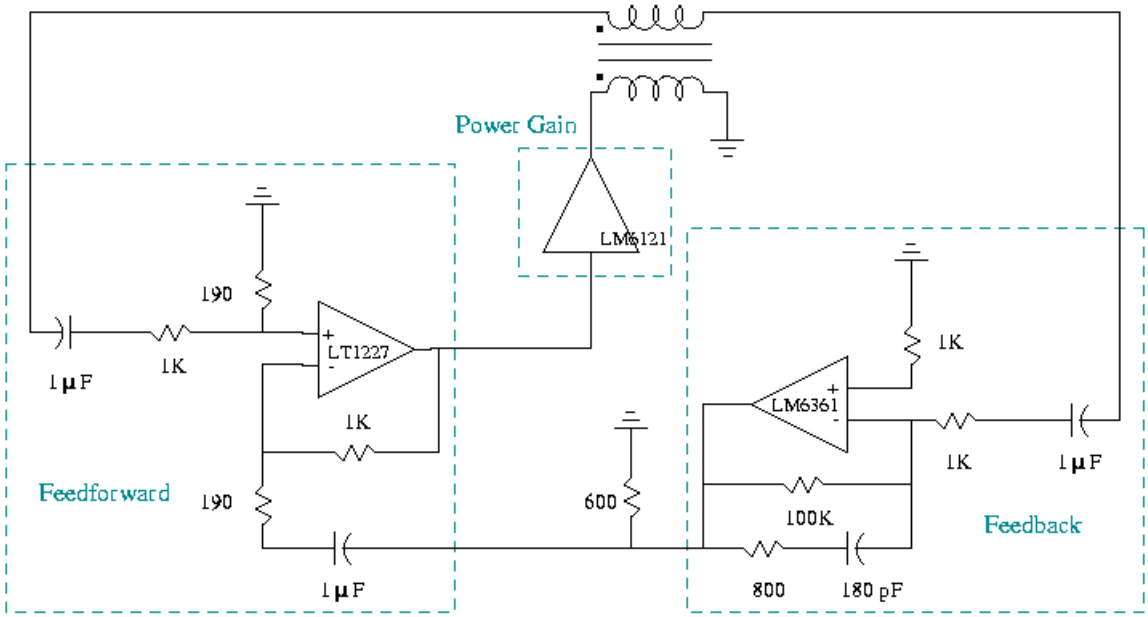

Figure 5 A three stage amplifier implementation of control. (From top to bottom and left to right.) The first stage provides the power gain to drive the injector transformer. The second stage serves as the feedforward gain and the summing point for the feedback control. The last stage is the feedback gain with minor-loop compensation.

implementation. The voltage injection attenuation with this approach may be calculated as:

$$Attenuation = \frac{N^2 L_u}{N^2 L_u + L_{l2}} \left(\frac{L_{DC}}{L_{l1} + L_{DC}}\right) = \frac{V_{out}}{V_{in}} \quad (7)$$

By minimizing the leakage inductances, L_{l1} and L_{l2}, the attenuation is minimized. It should be noted that in the previous case, only L_{l2} caused a magnitude error in the injected signal. In the two-core approach, L_{l1} also causes a magnitude error, because it forms a voltage divider with the bypass inductor. This approach can thus lead to a larger magnitude error.

The prototype ac transformer is wound on a non-gapped RM5 core. The combined volume of the inductor and transformer is 4884 mm^3. The single-core design has a volume of 8340 mm^3. This yields almost a 50% reduction in volume. The ac transformer magnetizing inductance L_m *is 50 mH*, L_{l1} leakage is 0.148 µH (or 0.4%) and the L_{l2} leakage inductance is 1.32µH (or 0.15%). This is much lower than in the previous design. However, the gain attenuation is increased, 0.92 as compared to 0.98 yielded by the single core design. The example confirms a volume verses gain tradeoff with the two magnetic component implementation in comparison to the single magnetic component implementation.

C. Active Circuitry Design

The design of the active circuit is greatly dependent upon the switching frequency of the dc/dc converter. The example power converter considered in this paper has a fundamental switching frequency of 125 KHz. Therefore to attenuate the fundamental and several of its harmonics the passband should include 100 KHz and beyond.

The active circuitry, illustrated in Fig 5, comprises a feedback amplifier, a feedforward amplifier that also acts as a summing amplifier for the feedback signal, and a power gain stage. The feedforward controller must be implemented with exact gain, minimal phase shift, and low distortion. The desired gain of the feedforward path is equal to the turns ratio divided by the attenuation caused by the transformer parasitics.

$$Gain_{single} = \frac{N^2 L_u + L_{l1}}{N L_u} \quad (8)$$

$$Gain_{two} = \frac{N^2 L_u + L_{l2}}{N L_u} \left(\frac{L_{l1} + L_{DC}}{L_{DC}}\right) \quad (9)$$

This way, the feedforward gain can be used to compensate the magnitude error due to transformer attenuation. The single core injector transformer requires a feedforward gain of 5, while the two-component injector requires a gain of 5.2, since its attenuation is larger.

A current feedback op-amp, LM1227, is used for the feedforward gain because it achieves the necessary gain, bandwidth, and slew-rate requirements for this application. The feedforward op-amp also acts as a summer, which allows this stage to incorporate the feedback control signal. A high-speed buffer, LM6121, is used to implement the power gain stage. It is able to provide +/- 100 mA of current with +/- 7 volt output swing at a bandwidth of 50 MHz. A high-frequency voltage-feedback op amp, LM6361, is used

for the feedback amplifier instead of a current feedback op amp because it simplifies the feedback control design. The LM361 has a predictable attenuation and phase shift.

There are two main limitations that dominate the feedforward system: non-exact gain compensation and nonzero amplifier output resistance. Due to parameter variations of the inductor and transformer, the feedforward gain cannot completely compensate for the magnitude error. Assuming zero phase error, the percentage error in magnitude corresponds directly to the percentage of residual ripple. For example, a 10% magnitude error results in a 10% residual ripple. The nonzero output impedance of the power gain stage causes a phase error, because it forms a high pass filter with the magnetizing inductance on the secondary side of the transformer.

$$\frac{V_{transformer}}{V_{circuit}} = \frac{sN^2L_u}{R_{out} + sN^2L_u} \qquad (10)$$

For perfect gain, the percentage of the residual ripple depends on the phase error ϕ in the following manner.

$$V_{residual} = \sqrt{(1-\cos f)^2 + \sin^2 j} \qquad (11)$$

The pole associated with the output resistance is at 6.4 KHz in the prototype. Although it is well below the fundamental frequency, there is a slight phase shift of 3 degrees at the switching frequency. This results in a maximum 95% ripple cancellation by the feedforward system, as per eqn. 11. The corresponding magnitude error is negligible. Therefore it is these errors in magnitude and phase that prevent perfect ripple nulling.

The design of the feedback controller is not only dependent on switching frequency, but also the stability of the control loop. The effectiveness of feedback control is directly dependent upon gain. Thus maximizing gain, without instability, is most desirable. As mentioned previously, the leakage inductance L_{l1} and the output capacitor C_{out} form a low pass filter, illustrated in Fig. 6. This two-pole filter causes an additional –180 degree phase shift from V_{sense} to V_{inject}. Neglecting damping and assuming that the buck capacitor is nearly ac ground, the

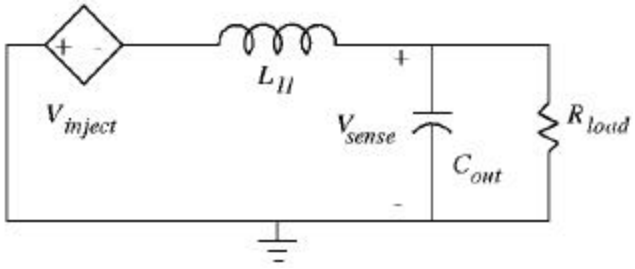

Figure 6 A circuit represention of the voltage injector loaded with the output capacitor. The voltage source represents the voltage transformer. To simplify the analysis the buck capacitor and the damping due to R_{load} has been neglected. The feedback signal is sensed across the ouptput capacitance.

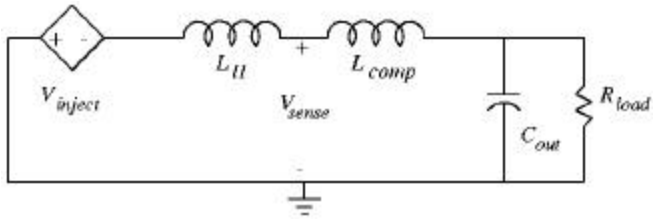

Figure 7 A circuit represention of the voltage injector loaded with the output capacitor and series compensating inductor. The voltage source represents the voltage transformer. To simplify the analysis the buck capacitor and the damping due to R_{load} has been neglected. The feedback signal is sensed between the two inductors.

following equation gives the transfer function from the transformer input to the output:

$$H_{injector}(s) = \frac{V_{sense}(s)}{V_{inject}(s)} = \frac{-1}{1+(L_{l1}C_{out})s^2} \qquad (12)$$

The higher the unity gain crossover frequency, the larger the gain will be across the frequency range of interest. However, if the –180 degree phase shift occurs before the unity-gain crossover, then the system will be unstable. Therefore, the parasitic low pass filter restricts the gain across the frequencies of interest, 125 KHz to 1MHz. This parasitic low pass filter occurs around 1.5 MHz in the prototype.

To overcome this limitation, a small inductive element, L_{comp}, is added between the sense point and the load, see Fig. 7. In the prototype system this was implemented as a small magnetic bead. This results in the addition of two zeros after the two poles.

$$H_{comp\_inj}(s) = \frac{V_{sense}(s)}{V_{inject}(s)} = \frac{-(L_{comp}C_{out})s^2 - 1}{s^2(L_{comp}+L_{l1})C_{out} + 1} \qquad (13)$$

If L_{comp} is much smaller than L_{l1} then the zeros occur just after the poles. Therefore the phase of the system approaches –180 degrees (never reaching it due to damping) and then returns to zero degrees. Fig 9 shows the frequency response of $H_{comp\_inj}(s)$ for the prototype system.

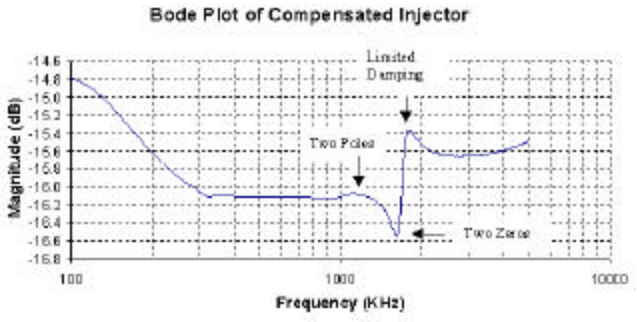

Figure 9 The transfer function of the voltage injection system. The two poles due to the low pass filter formed by L_{l1}+L_{comp} and C_{out} adds a –180 phase shift. $Lcomp$ adds the two zeros and C_{out} brings the phase back to 0 degree. The magnitude shows peaking near the poles and zeros of the system, which is due to limited damping.

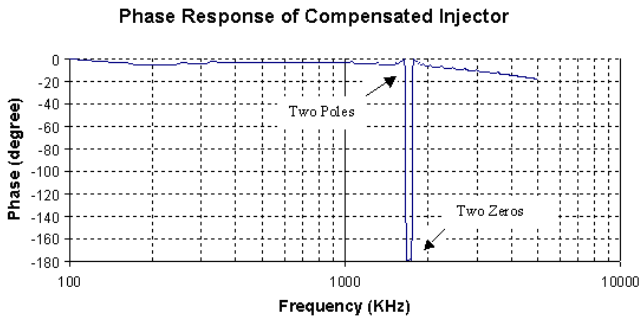

Figure 9 The transfer function of the voltage injection system. The two poles due to the low pass filter formed by L_{l1}+L_{comp} and C_{out} adds a –180 phase shift. *Lcomp* adds the two zeros and C_{out} brings the phase back to 0 degree. The magnitude shows peaking near the poles and zeros of the system, which is due to limited damping.

The attenuation of the ripple will be greatly degraded at the frequency where the minimum of magnitude response occurs. Furthermore, the ripple at this frequency is greater with feedback filtering than without. This is because not only is the magnitude at a minimum but the phase is nearly (–180) degrees, which makes the gain, *A(s)*, a negative number less than one, thus causing the attenuation to become less than one. Despite all this, the gain can be increased, because the unity gain cross over frequency extends pass 1.5 MHz. The small ferrite bead used as the compensation inductance in the prototype not only adds inductance but extra resistive damping. This allows the unity gain frequency to occur at 10 MHz. Minor loop compensation is used to further increase stability. The gain of the current system is 50 at 125 KHz and decreases 20 dB per decade. Since the gain is not infinite, the feedback controller is not able to completely eliminate the ripple.

D. Sensor Design

Both feedback and feedforward signals are sensed using high-pass filters feeding directly in to the gain amplifiers.

This implementation proves to be efficient and straightforward for sensing ac signals, while rejecting the dc component. The pole of each filter is placed well below the fundamental ripple frequency to reduce magnitude and phase errors. Placing the pole a factor of 100 below the fundamental switching frequency gives about 0.6 degrees of phase shift at the fundamental. The prototype has the poles about a factor of 700 below the fundamental switching frequency; the corresponding phase shift is only 0.07 degrees.

III. EXPERIMENTAL RESULTS

The proposed hybrid passive/active filter technique has been applied to the design of an output filter for a 230 watt buck converter operating at 14 V output from a 42 V nominal input (Fig. 10). The fundamental switching frequency is 125 KHz. The buck converter power stage utilizes a 1.4 μH inductor and 20 μF primary output capacitor and operates in discontinuous conduction mode under average current mode control.

A structural view of the output filter and test setup is shown. The passive component of the hybrid filter comprises a 0.2 μF ceramic capacitor and a damping leg made up of a 1 μF electrolytic capacitor and a 0.22 Ω resistor. The damping leg can also be implemented with a simple active element, if desired. Tests of the system were conducted using conventional EMI test procedures. A Line Impedance Stabilization Network (LISN) was placed between the load and the output filter. Tests described here were performed using a 1 Ω load. The LISN passes power frequency signals to the load, while acting as a known impedance at ripple frequencies. The voltage across the 50 ohm LISN resistor is used as the metric for output ripple performance.

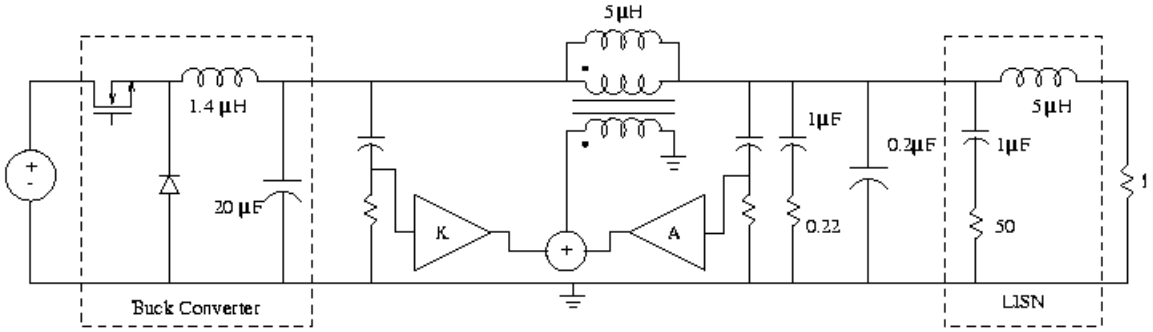

Figure 10 Test setup for the hybrid filter. Active filter is used in conjunction with a smaller passive output filter. The reduced output filter consists of a 0.2 μF capacitor with a damping leg of a 0.22 Ω resistor and a 1 μF electrolytic capacitor.

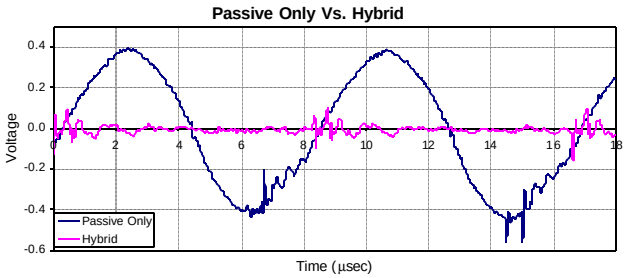

Figure 11 The experimental test results for a 125 KHz buck converter. The above graph shows the voltage ripple measured at the LISN. Peak to peak ripple is greatly reduced by the active circuit.

Measurements were first taken without injection from the active filter element. Essentially, the 5 µH magnetizing inductance of the injector transformer and the 0.2 µF output capacitor forms a conventional LC low-pass filter. Measurements were then taken with the active filter in operation. Figure 11 illustrates the dramatic improvement in output voltage ripple performance that is achieved through the use of the active filter. The spectral measurements of Fig. 12 indicate that the use of active injection provides almost 35 dB reduction in fundamental ripple voltage and results in the largest component across frequency being 25 dB lower in magnitude.

As mentioned previously, the best results are achieved with feedforward and feedback control used together, as illustrated in Fig. 13. Individually, the feedforward and feedback controls above are able to achieve about 20 dB ripple attenuation, corresponding to about 10% residual ripple. The amount of attenuation attainable for feedforward is limited by phase and magnitude error. The feedforward control has very slight magnitude and phase errors, but they significantly limit feedforward ripple cancellation. Stability considerations limit achievable feedback gain and ripple attenuation. The ripple around 700 KHz is greater with

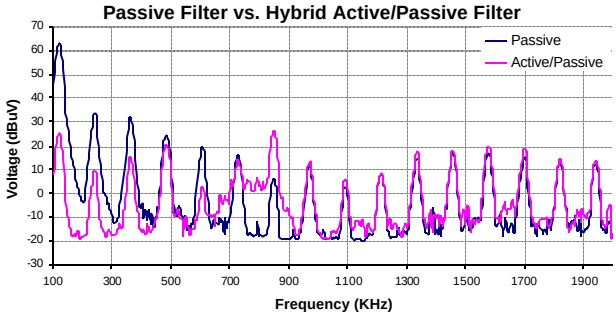

Figure 12 Ripple spectra measured at the output of the LISN for both the hybrid active/passive filter and a small passive filter of the same size. The hybrid filter achieves a 35 dBµV attenuation of the fundamental ripple frequency; see Fig. 13 for comparison.

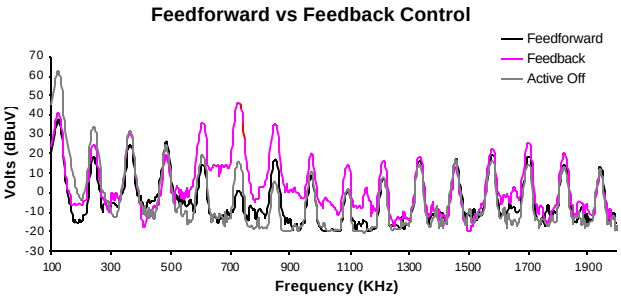

Figure 13 Ripple spectra measured at the output of the LISN for both feedforward and feedback control used individually. The measurement with the active filter off is offered for comparison. Each control has its own performance limitations. The feedback control actually performs worse than no active filtering at certain frequencies.

feedback ripple cancellation than without, reflecting deterioration in filter performance in this region due to ripple *amplification* by the feedback. The increase in ripple from feedback control in the region is compensated by the feedforward control. Therefore, as illustrated in Fig. 12, the combination of the two control systems yields a superior result over either one alone. Essentially, the two control schemes work together to achieve superior attenuation at the fundamental. At higher frequencies the feedforward controller compensates for the limitations of the feedback controller.

In order to compare the benefits of hybrid filters to conventional passive filter design methods, a passive filter meeting the same ripple specification is designed using the 5 µH magnetizing inductance of the injector. The larger passive filter requires a 20 µF capacitor to meet the same ripple specification across frequency (ripple ≤ 25 dBµV across frequency). Relative performance of the hybrid filter and large passive filter is shown in Fig. 14. Therefore the hybrid filter allows a 20 µF capacitor to be replaced with a 0.2 µF capacitor with no degradation in performance. This corresponds to a factor of 100 reduction in the required filter capacitance utilizing the hybrid active/passive approach presented here. Thus the benefit of the proposed approach is that by introducing simple, signal-level active circuitry along with an additional passive inductor winding (or small ac transformer), one can dramatically reduce the passive filter capacitance for the same level of performance.

IV. CONCLUSION

Active ripple filters can affect substantial reductions in power converter input and output ripple components, allowing considerable reduction in passive component size. This paper investigates a hybrid passive/active filter topology that achieves ripple reduction by injecting a compensating voltage ripple across a series filter element.

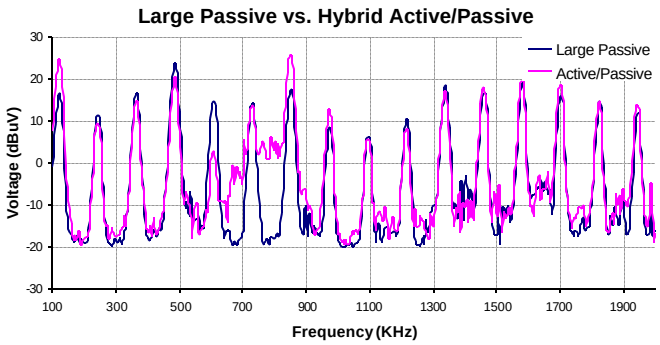

Figure 14 LISN voltage spectra of the hybrid active/passive filter and a large passive filter with a 20 µF capacitor. The plots indicate that both the hybrid filter and the large passive filter both meet a flat 25 dBµV ripple specification across frequency.

Both ripple feedforward and feedback are employed. The design of sensor, amplifier, and injector circuitry suitable for the application are investigated. The experimental results demonstrate the feasibility and high performance of the new approach, and illustrate its potential benefits. It is demonstrated that the proposed approach is most effective in cases where it is desirable to minimize the amount of capacitance in the filter. In these cases, a reduction of a factor of 100 or more is possible with the active filter, without impacting ripple performance.

ACKNOWLEDGEMENTS

The authors would like to acknowledge the support for this research provided by the United States Office of Naval Research under grant number N00014-00-1-0381, and by the member companies of the MIT/Industry Consortium on Advanced Automotive Electrical/Electronic Components and Systems.

REFERENCES

[1] T.K. Phelps and W.S. Tate, "Optimizing Passive Input Filter Design," *Proceedings of Pwercon 6*, May 1979, pp. G1-1 - G1-10.

[2] M. Zhu, D.J. Perreault, V. Caliskan, T.C. Neugebauer, S. Guttowski, and J.G. Kassakian, "Design and Evaluation of an Active Ripple Filter with Rogowski-Coil Current Sensing," *IEEE PESC Rec.*, Vol. 2, 1999, pp. 874 -880 vol.2.

[3] S. Feng , W. A. Sander, and T. Wilson, "Small-Capacitance Nondissipative Ripple Filters for DC Supplies," *IEEE Trans. Mag.*, Vol.6, N0. 1, March 1970, pp. 137-142.

[4] D.C. Hamill "An Efficient Active Ripple Filter for Use in DC-DC Conversion," *IEEE Trans. Aero. and Electron. Sys.*, Vol. 32, No3, July 1996, pp. 1077-1084.

[5] N.K. Poon, J.C.P. Liu, C.K. Tse, and M.H Pong, "Techniques for Input Ripple Current Cancellation: Classification and Implementation," *IEEE T POWER ELECTR*, Vol. 15, No. 6, NOV 2000, pp. 1144-1152.

[6] J. Walker, "Designing Practical and Effective Active EMI filters," *Proceedings of Powercon 11*, 1984, I-3 pp. 1-8.

[7] L.E. LaWhite and M.F. Schlecht, "Active Filters for 1 MHz Power Circuits With Strict Input/Output Ripple Requirements," *IEEE Trans. Power Electron.*, Vol. PE-2, No.4, Oct. 1987, pp. 282-290.

[8] T. Farkas and M.F. Schlecht, "Viability of Active EMI Filters for Utility Applications," *IEEE T POWER ELECTR*, Vol. 9, No. 3, MAY 1994, pp. 328-337.

[9] M.S. Moon and B.H. Cho "Novel Active Ripple Filter for the Solar Array Shunt Switching Unit," *J PROPUL POWER*, Vol. 12, No. 1, JAN-FEB 1996, pp. 78-82.

[10] P. Midya and P.T. Krein, "Feed-forward Active Filter for Output Ripple Cancellation," *Int. J. Elec.*, Vol. 77, No. 5, pp. 805-818.

[11] L.R. Casey, A. Goldberg, and M.F. Schlecht, "Issues Regarding the Capacitance of 1-10 MHz Transformers," *Proc. IEEE APEC*, 1988 pp. 352 –359.

[12] A. Goldberg, J.G. Kassakian, and M.F. Schlecht, "Issues Related to 1-10-MHZ Transformer Design," *IEEE Tran. Power Electron.*, Vol. 4, No. 1, JAN 1989, pp. 113-123.